An NLO calculation of the electroproduction of large $E_\perp$ hadrons

Rahul Basu

The Institute of Mathematical Sciences

Taramani, Chennai 600 113

India

http://www.imsc.res.in/~rahul

with P. Aurenche, M. Fontannaz and R. Godbole

Deep Inelastic Scattering at HERA

$e^+ - P$ collider machine which reached very small values of Bjorken x:

$e(k) + P(p) \rightarrow e(k') + X$

The following kinematic variables completely describe the process:

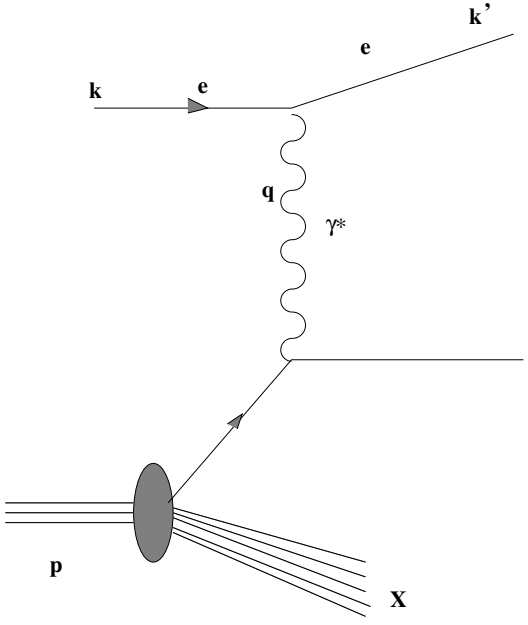

$$
\begin{aligned}
s = (k+p)^2 &\simeq 4E_e E_p \\
Q^2 = -q^2 &\simeq 2E_e E_{e'}(1 + cos\theta) \\
y = \frac{p.q}{p.k} &\simeq 1 - \frac{E_{e'}}{2E_e}(1 - cos\theta) \\
x = \frac{Q^2}{2p.q} &\simeq \frac{Q^2}{ys} \\
W = (q+p)^2 &\simeq -Q^2 + ys
\end{aligned}
$$

HERA has provided an unprecedented view into the structure of the proton at low x and large Q^2. Agreement with theory is phenomenally (and misleadingly) perfect! Looking at purely inclusive measurement F_2.

Forward Jets and Single Particle Production

The cross section for forward jet production in DIS was suggested by Mueller (Mueller 1991, Mueller, Navelet 1991) as a means of distinguishing these different resummation schemes.

Forward Jets and Single Particle Production

The cross section for forward jet production in DIS was suggested by Mueller (Mueller 1991, Mueller, Navelet 1991) as a means of distinguishing these different resummation schemes.

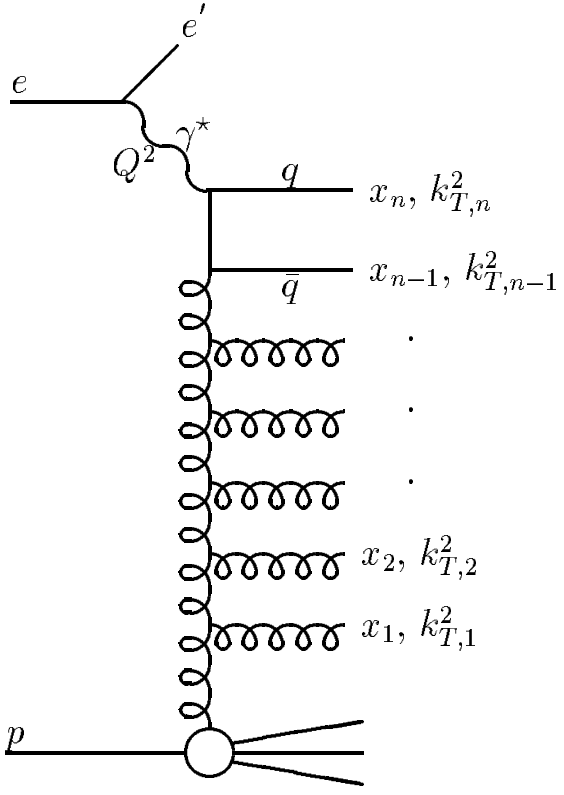

Forward Jets and Single Particle Production

The cross section for forward jet production in DIS was suggested by Mueller (Mueller 1991, Mueller, Navelet 1991) as a means of distinguishing these different resummation schemes.

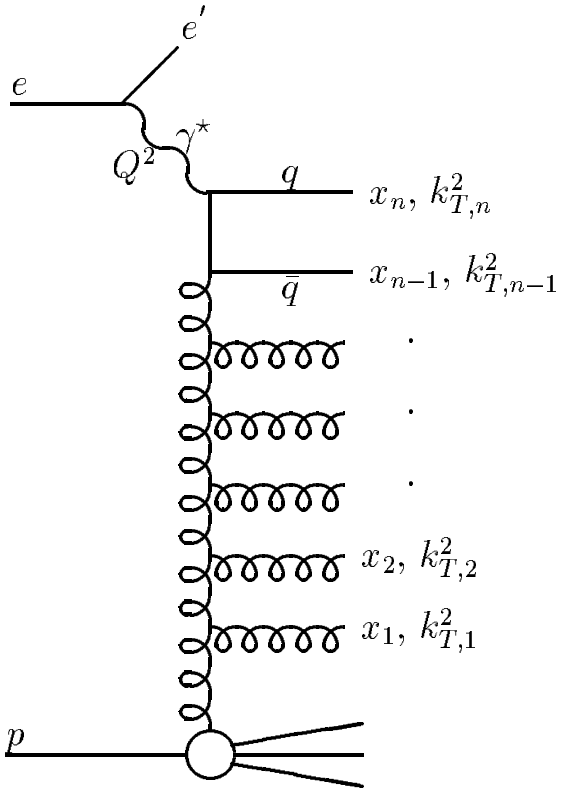

DGLAP and BFKL predict different ordering of the transverse momenta $k_{T,i}$ along the parton cascade developing in DIS jet production. DGLAP predicts strong $k_{T,i}$ ordering ($Q^2 = k^2_{T,n} \gg \ldots k^2_{T,1}$) whereas BFKL predicts strong ordering in x_i, $x \ll x_n \ldots \ll x_1$.

Observe jets at small x in the forward region $Q^2 \simeq k^2_{T,1} \Rightarrow$ DGLAP evolution suppressed and BFKL evolution left active.

Forward Jets and Single Particle Production

The cross section for forward jet production in DIS was suggested by Mueller (Mueller 1991, Mueller, Navelet 1991) as a means of distinguishing these different resummation schemes.

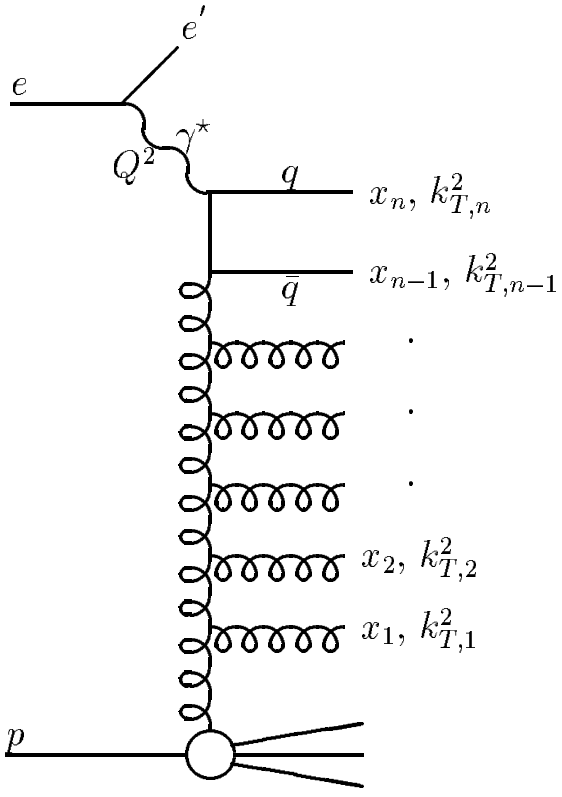

DGLAP and BFKL predict different ordering of the transverse momenta $k_{T,i}$ along the parton cascade developing in DIS jet production. DGLAP predicts strong $k_{T,i}$ ordering ($Q^2 = k^2_{T,n} \gg \ldots k^2_{T,1}$) whereas BFKL predicts strong ordering in x_i, $x \ll x_n \ldots \ll x_1$.

Observe jets at small x in the forward region $Q^2 \simeq k^2_{T,1} \Rightarrow$ DGLAP evolution suppressed and BFKL evolution left active.

Hadronic final state quantities are sensitive to the dynamics of QCD processes and are thus expected to be able to discriminate between different evolution approximations.

Hadronic Final State Quantities

- Forward Jet Production:
  studied through leading order BFKL and also NLO fixed order ; various Monte Carlo models (ARIADNE, LEPTO, HERWIG, RAPGAP, LDC) implementing these have been used to compare the date with theoretical predictions. Unfortunately, both BFKL and NLO fixed order QCD calculations can be used to describe the data reasonably well.

Hadronic Final State Quantities

- Forward Jet Production:
  studied through leading order BFKL and also NLO fixed order ; various Monte Carlo models (ARIADNE, LEPTO, HERWIG, RAPGAP, LDC) implementing these have been used to compare the date with theoretical predictions. Unfortunately, both BFKL and NLO fixed order QCD calculations can be used to describe the data reasonably well.

- Single Particle Production:
  Avoids various uncertainties of forward jet production $\Rightarrow$ jet algorithms, but has been studied only at LO which severely underestimates the data $\Rightarrow$ need to go to NLO to make any definite statements with regard to comparison with data.

NLO calculation of large $p_\perp$ hadrons in DIS

The calculations consists of various steps needed to finally define an Infrared Safe Observable.

- The Born level partonic cross section $\gamma^* + q \rightarrow g + q$, $\gamma^* + g \rightarrow q + \bar{q}$

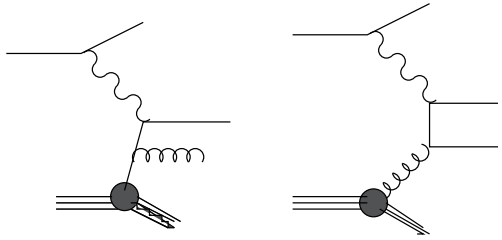

NLO calculation of large $p_\perp$ hadrons in DIS

The calculations consists of various steps needed to finally define an Infrared Safe Observable.

- The Born level partonic cross section $\gamma^* + q \rightarrow g + q$, $\gamma^* + g \rightarrow q + \bar{q}$

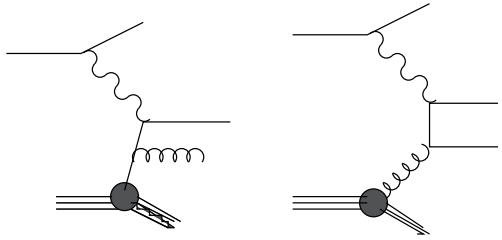

- The Higher Order Correction terms are of the form (real) $\gamma^* + q \rightarrow q + g + g$, $\gamma^* + g \rightarrow q + \bar{q} + g \ldots$

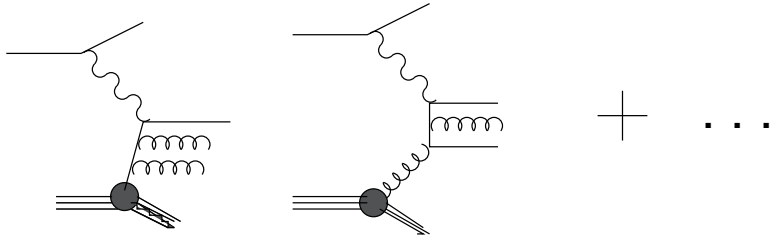

NLO calculation of large $p_\perp$ hadrons in DIS

The calculations consists of various steps needed to finally define an Infrared Safe Observable.

- The Born level partonic cross section $\gamma^* + q \rightarrow g + q$, $\gamma^* + g \rightarrow q + \bar{q}$

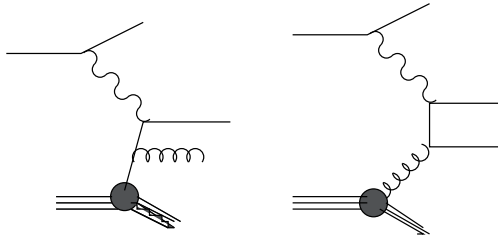

- The Higher Order Correction terms are of the form (real) $\gamma^* + q \rightarrow q + g + g$, $\gamma^* + g \rightarrow q + \bar{q} + g \ldots$

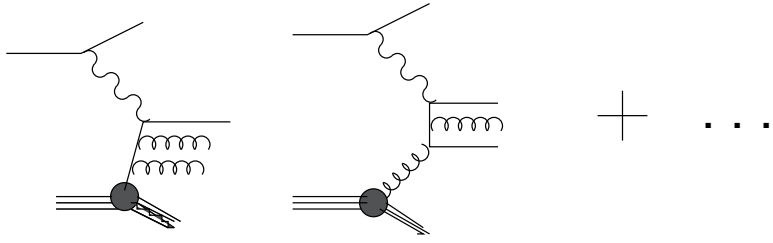

- And the virtual diagrams

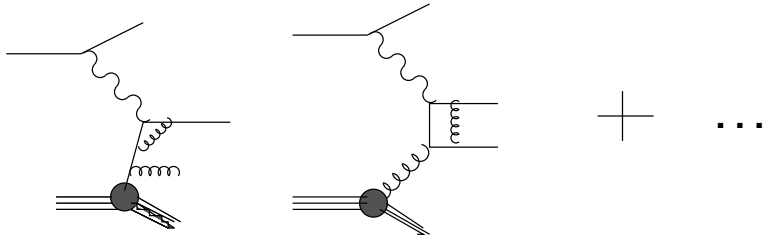

IR problems

- Like all QCD calculations, both real and virtual corrections exhibit infrared singularities which have to be cancelled/absorbed into distribution functions.

IR problems

- Like all QCD calculations, both real and virtual corrections exhibit infrared singularities which have to be cancelled/absorbed into distribution functions.
- For our general $2 \to 3$ partonic subprocess, virtual and real emission diagrams give various singularities.

IR problems

- Like all QCD calculations, both real and virtual corrections exhibit infrared singularities which have to be cancelled/absorbed into distribution functions.
- For our general $2 \to 3$ partonic subprocess, virtual and real emission diagrams give various singularities.
- Collinear singularities appear as $\frac{1}{\epsilon}$ divergences in Dim. Reg. Scheme. Infrared (soft) divergences appear at this order as $\frac{1}{\epsilon^2}$

IR problems

- Like all QCD calculations, both real and virtual corrections exhibit infrared singularities which have to be cancelled/absorbed into distribution functions.
- For our general $2 \to 3$ partonic subprocess, virtual and real emission diagrams give various singularities.
- Collinear singularities appear as $\frac{1}{\epsilon}$ divergences in Dim. Reg. Scheme. Infrared (soft) divergences appear at this order as $\frac{1}{\epsilon^2}$
- $\frac{1}{\epsilon^2}$ pieces cancel when real and virtual diagrams are added. $\frac{1}{\epsilon}$ pieces are absorbed into evolved structure functions (for initial state particles) or evolved fragmentation functions (for final state radiation).

IR problems

- Like all QCD calculations, both real and virtual corrections exhibit infrared singularities which have to be cancelled/absorbed into distribution functions.
- For our general $2 \to 3$ partonic subprocess, virtual and real emission diagrams give various singularities.
- Collinear singularities appear as $\frac{1}{\epsilon}$ divergences in Dim. Reg. Scheme. Infrared (soft) divergences appear at this order as $\frac{1}{\epsilon^2}$
- $\frac{1}{\epsilon^2}$ pieces cancel when real and virtual diagrams are added. $\frac{1}{\epsilon}$ pieces are absorbed into evolved structure functions (for initial state particles) or evolved fragmentation functions (for final state radiation).
- To carry out this procedure we need a systematic method to extract all these divergences.

General structure of the cross section

Kinematics of the general reaction:

$$e(\ell) + p(P) \rightarrow e(\ell') + h(P_4) + X$$

fixed by momenta of the outgoing lepton and the hadron h (transverse momentum p_{T4} and pseudo rapidity η_4).

$$\frac{d\sigma}{d\varphi dQ^2 dy dE_{\perp 4} d\eta_4} = \frac{\alpha}{2\pi} \sum_{a,b} \int dx G_a(x, M) \int \frac{dz}{z^2} D_b^h(z, M_F)$$

$$\left\{ \frac{\alpha_s(\mu)}{2\pi} \frac{d\widehat{\sigma}_{a,b}^{Born}(x,z)}{d\varphi dQ^2 dy dE_{\perp 4} d\eta_4} + \left(\frac{\alpha_s(\mu)}{2\pi} \right)^2 \frac{dK_{ab}^{HO}(x, z, \mu, M, M_F)}{d\varphi dQ^2 dy dE_{\perp 4} d\eta_4} \right\}$$

$\widehat{\sigma}_{a,b}^{Born}(x,z)$ are the subprocess Born cross sections describing the production of a large-p_T parton b and K_{ab}^{HO} are the associated Higher Order corrections.

In actual practise, $\widehat{\sigma}_{a,b}^{Born}(x,z)$ and K_{ab}^{HO} are calculated in the virtual photon - proton CMS frame since the H1 collaboration explicitly uses this frame to place cuts on the outgoing hadron transverse momentum.

Regulating IR divergences in our case

A combination of Phase-space slicing and Subtraction methods is used.

Consider the generic process $1 + 2 \rightarrow 3 + 4 + 5$

Only one of the final state particles can be soft (say 5) and the others 3 and 4 have a high p_T and are well separated in phase space.

Thus, 5 can be soft, or collinear to any of the four other particles.

The phase space is now sliced using two arbitrary unphysical parameters p_{Tm} and R_{th}

Regulating IR divergences contd. . .

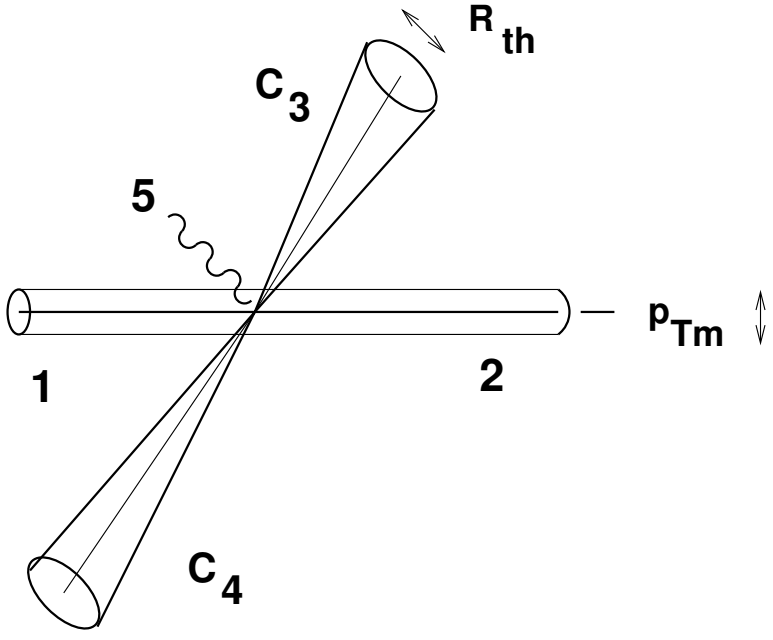

- Part I: $|p_{T5}| < p_{Tm} \ll$ other transverse momenta. This cylinder supplies the IR and initial state collinear singularities (and a small fraction of the final state collinear singularities).

Regulating IR divergences contd...

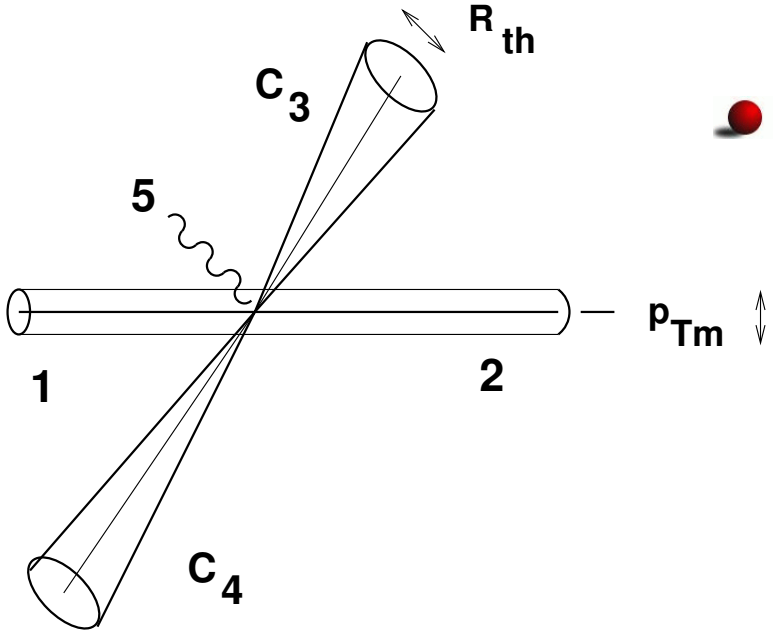

- Part I: $|p_{T5}| < p_{Tm} \ll$ other transverse momenta. This cylinder supplies the IR and initial state collinear singularities (and a small fraction of the final state collinear singularities).
- Part IIa:$|p_{T5}| > p_{Tm}$ and belongs to a cone C_3 about direction of 3 $(y_5 - y_3)^2 + (\phi_5 - \phi_3)^2 \leq R_{th}^2$. C_3 contains the final state collinear singularities for $5//3$

Regulating IR divergences contd...

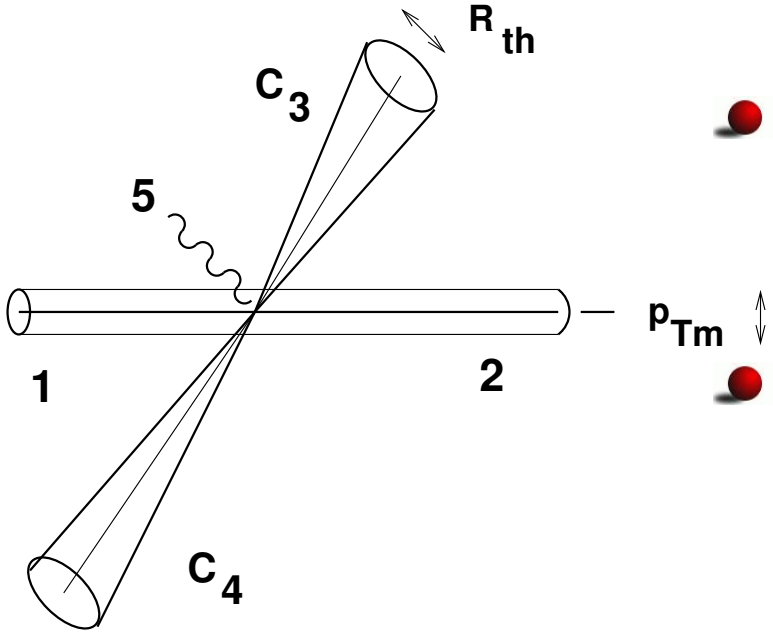

- Part I: $|p_{T5}| < p_{Tm} \ll$ other transverse momenta. This cylinder supplies the IR and initial state collinear singularities (and a small fraction of the final state collinear singularities).
- Part IIa:$|p_{T5}| > p_{Tm}$ and belongs to a cone C_3 about direction of 3
  $(y_5 - y_3)^2 + (\phi_5 - \phi_3)^2 \leq R_{th}^2$. C_3 contains the final state collinear singularities for $5//3$
- Part IIb:$|p_{T5}| > p_{Tm}$ and belongs to a cone C_4 about direction of 4
  $(y_5 - y_4)^2 + (\phi_5 - \phi_4)^2 \leq R_{th}^2$. C_4 contains the final state collinear singularities for $5//4$

Regulating IR divergences contd...

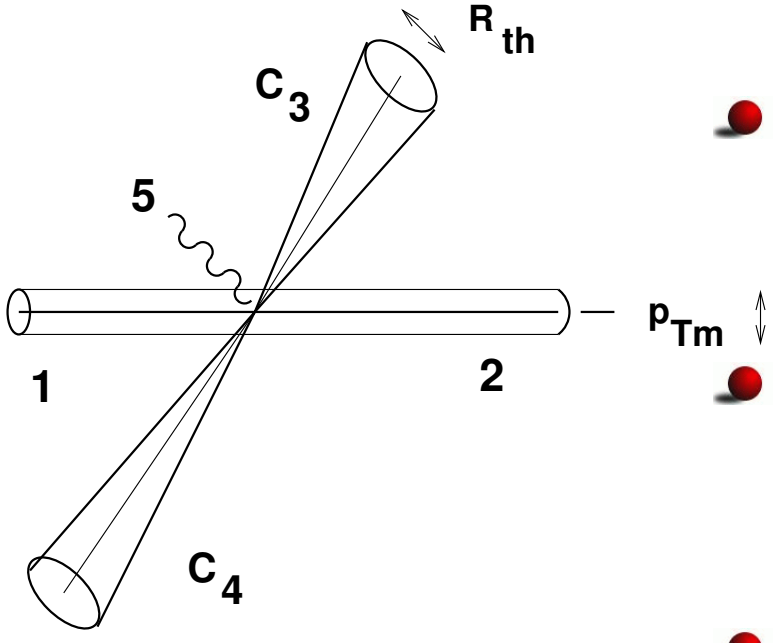

- Part I: $|p_{T5}| < p_{Tm} \ll$ other transverse momenta. This cylinder supplies the IR and initial state collinear singularities (and a small fraction of the final state collinear singularities).
- Part IIa:$|p_{T5}| > p_{Tm}$ and belongs to a cone C_3 about direction of 3
  $(y_5 - y_3)^2 + (\phi_5 - \phi_3)^2 \leq R_{th}^2$. C_3 contains the final state collinear singularities for $5//3$
- Part IIb:$|p_{T5}| > p_{Tm}$ and belongs to a cone C_4 about direction of 4
  $(y_5 - y_4)^2 + (\phi_5 - \phi_4)^2 \leq R_{th}^2$. C_4 contains the final state collinear singularities for $5//4$
- Part IIc:$|p_{T5}| > p_{Tm}$ and belongs to neither of the two cones C_3 or C_4. This part has no divergence and can be treated directly in 4 dimensions.

IR divergences contd. . .

- Divergent contributions from regions I, IIa,b are calculated analytically in $d = 4 - 2\epsilon$ and combined with the virtual terms.

IR divergences contd. . .

- Divergent contributions from regions I, IIa,b are calculated analytically in $d = 4 - 2\epsilon$ and combined with the virtual terms.
- IR divergences cancel, initial (final) state coll. singularities absorbed into parton distribution (fragmentation) functions.

IR divergences contd. . .

- Divergent contributions from regions I, IIa,b are calculated analytically in $d = 4 - 2\epsilon$ and combined with the virtual terms.
- IR divergences cancel, initial (final) state coll. singularities absorbed into parton distribution (fragmentation) functions.
- Finite remainders of I, IIa,b,c are calculated using a MC integration. These depend on $\ln p_{Tm}$, $\ln^2 p_{Tm}$ for region I and $\ln R_{th}$ for region II a,b.

IR divergences contd. . .

- Divergent contributions from regions I, IIa,b are calculated analytically in $d = 4 - 2\epsilon$ and combined with the virtual terms.
- IR divergences cancel, initial (final) state coll. singularities absorbed into parton distribution (fragmentation) functions.
- Finite remainders of I, IIa,b,c are calculated using a MC integration. These depend on $\ln p_{Tm}$, $\ln^2 p_{Tm}$ for region I and $\ln R_{th}$ for region II a,b.
- Terms proportional to p_{Tm} and R_{th} are dropped (small). The log terms cancel when all the parts are combined (p_{Tm} and R_{th} are chosen small but not too small to prevent numerical instabilities).

Results

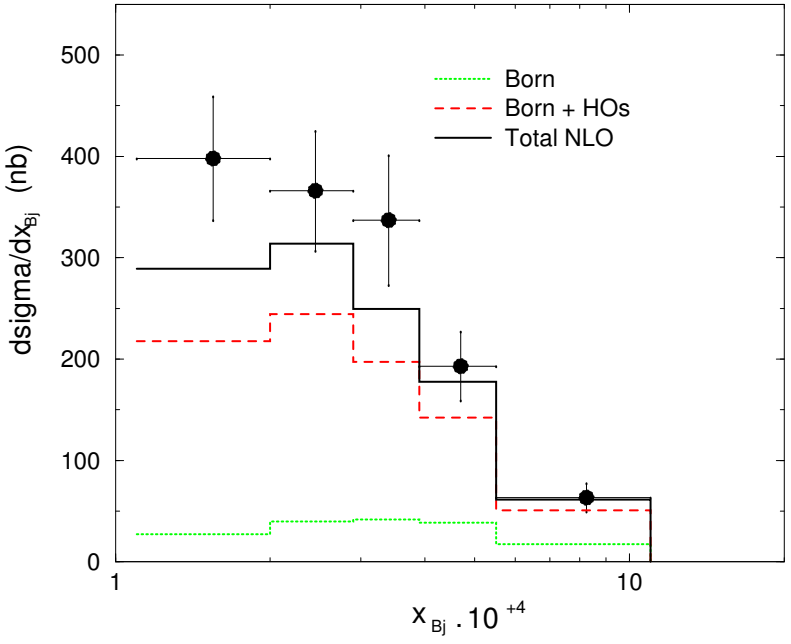

$4.5\ \text{GeV}^2 \leq Q^2 \leq 15\ \text{GeV}^2$

$p_T^* > 2.5$ GeV

$.1 < y < .6$

$5^\circ \leq \theta_\pi^{Lab} \leq 25^\circ$

$x_\pi = E_\pi^{Lab}/E_{proton}^{Lab} \geq .01$

Size of the HO corrections is large, particularly at low x_{Bj} (opening of new channels). $HO_s \Rightarrow$ HO contributions from where the resolved contribution has been subtracted out. (will return to this later)

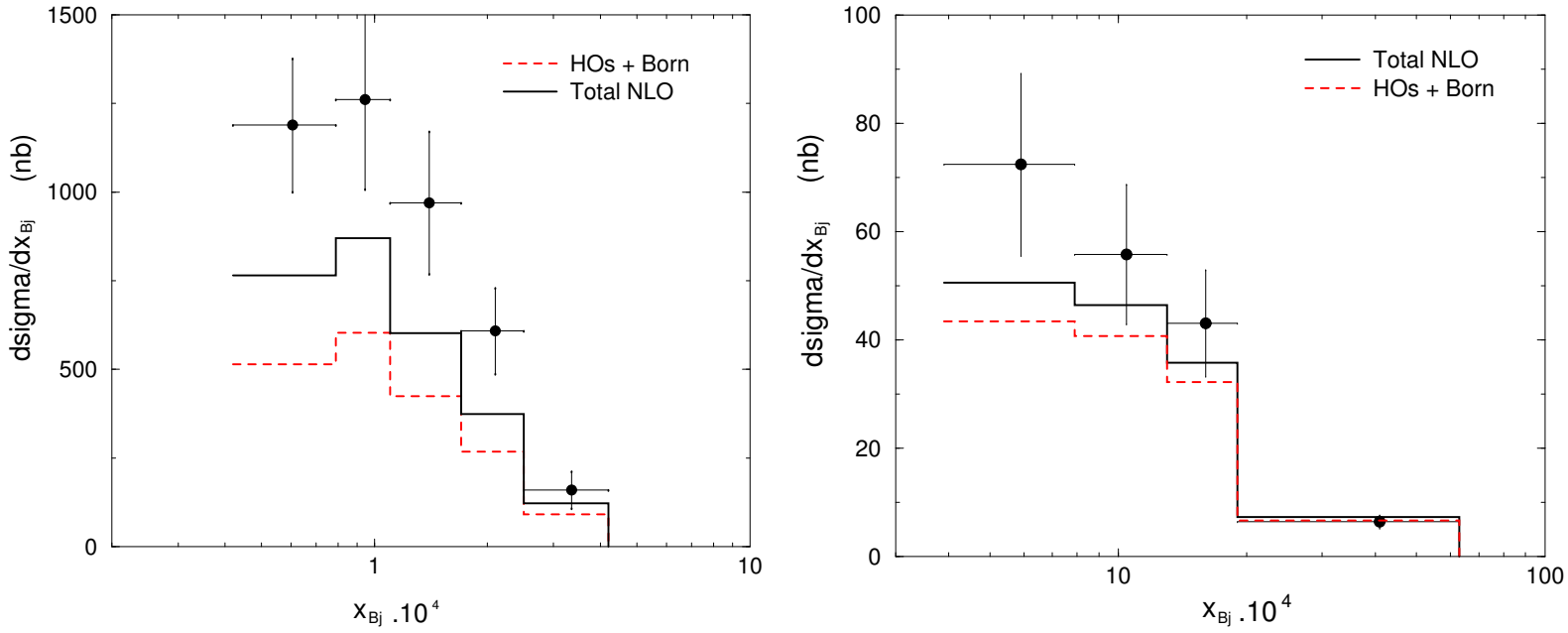

Data and results for $2 < Q^2 < 4.5$GeV^2 and $15 < Q^2 < 70$GeV^2 Note that the resolved component decreases when Q^2 increases as also when x_{Bj} increases.

Resolved Photon contribution

HO correction $\Rightarrow$ contains contribution proportional to $\ln \frac{E^2_{\perp 4}}{Q^2}$ when $E^2_{\perp 4} \gg Q^2$ $\Rightarrow$ from integration over $p_{\perp 5}$ – the unobserved final quark momentum $\Rightarrow$ from configuration in which the final quark is collinear to the virtual photon. In fact, for the $2 \rightarrow 2$ process

$$\sigma_\perp \simeq \int dz P_{q\gamma}(z) \left\{ \log \frac{E^2_{\perp 4}}{Q^2} \right\} \widehat{\sigma}(0)\, dps$$

with $P_{q\gamma}(z) = \frac{\alpha}{2\pi}(z^2 + (1-z)^2)$ and the quark distribution in the virtual photon

$$q_\gamma(z, E_{\perp 4}, Q^2) = P_{q\gamma}(z)\ \log \frac{E^2_{\perp 4}}{Q^2}$$

Resolved Photon Contribution $\Rightarrow$ calculated in the pure QED limit. When $E^2_{\perp 4} \gg Q^2$ need to include LO or NLO QCD corrections (because terms like $\alpha_s \ln \frac{E^2_{\perp 4}}{Q^2}$ appear. However in the kinematical configuration of the H1 experiment, this lowest order expression is sufficient. The resolved photon contribution dies out with increasing virtuality of the photon and goes as

$$\sigma_\perp \simeq \int dz P_{q\gamma}(z) \left\{ \log \frac{E^2_{\perp 4} + Q^2}{Q^2} \right\} \widehat{\sigma}(0)\, dps$$

Results contd. . .

- Theory underestimates data by a small amount

Results contd. . .

- Theory underestimates data by a small amount
- We need to consider the scale dependence of the results (which here have been calculated at $\mu = M = M_F = (Q^2 + E_{\perp 4}^2)^{1/2}$)

Results contd. . .

- Theory underestimates data by a small amount
- We need to consider the scale dependence of the results (which here have been calculated at $\mu = M = M_F = (Q^2 + E_{\perp 4}^2)^{1/2}$)
- We need to look at the HO corrections to the resolved part which are large - this when included gives $HO/Born \simeq 1$ in the kinematical domain of the graphs shown

Resolved Contribution - HO

Recently Michel Fontannaz has calculated the HO corrections to the resolved part

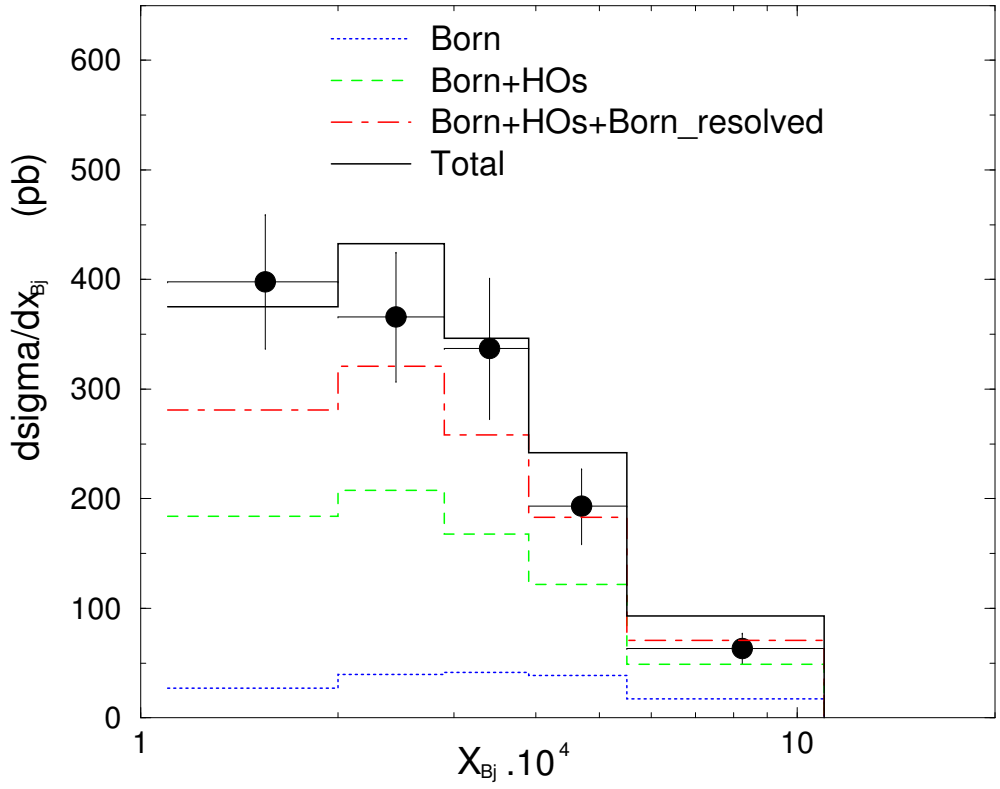

Clearly the HO correction to the resolved piece can be substantial $\Rightarrow$ affects the scale needed to match the data compared with just taking the lowest order (Born) resolved piece.

Some details of the HO corrections

- The two largest contributions come from

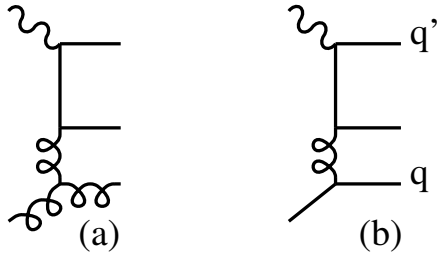

$\Rightarrow$ exchange of a gluon in the t-channel.

Some details of the HO corrections

- The two largest contributions come from

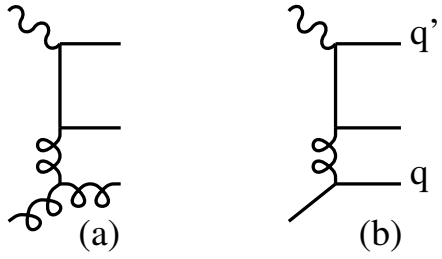

  $\Rightarrow$ exchange of a gluon in the t-channel.

- These are qualitatively new subprocesses not present at the Born level *i.e.* they do not possess singular configurations of partons which contribute to the dressing up of the distribution (fragmentation) functions already present in the Born term.

Some details of the HO corrections

- The two largest contributions come from

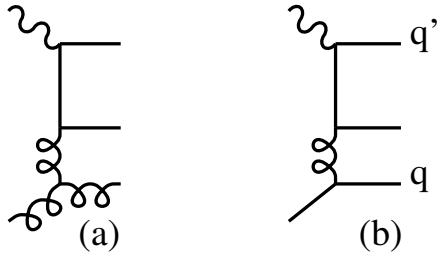

  $\Rightarrow$ exchange of a gluon in the t-channel.

- These are qualitatively new subprocesses not present at the Born level *i.e.* they do not possess singular configurations of partons which contribute to the dressing up of the distribution (fragmentation) functions already present in the Born term.

- $\Rightarrow$ These graphs (with a trigger on the g or q but *not* on q') are the lowest order BFKL terms in which extra gluons are emitted by the t-channel gluon

Some details of the HO corrections

- The two largest contributions come from

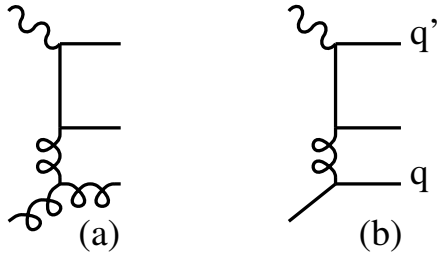

  $\Rightarrow$ exchange of a gluon in the t-channel.

- These are qualitatively new subprocesses not present at the Born level *i.e.* they do not possess singular configurations of partons which contribute to the dressing up of the distribution (fragmentation) functions already present in the Born term.
- $\Rightarrow$ These graphs (with a trigger on the g or q but *not* on q') are the lowest order BFKL terms in which extra gluons are emitted by the t-channel gluon
- These, therefore contribute precisely to the forward cross section that HERA experiments are supposed to study to reveal BFKL dynamics

Some details of the HO corrections

- The two largest contributions come from

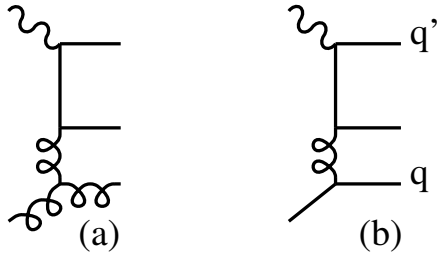

  $\Rightarrow$ exchange of a gluon in the t-channel.

- These are qualitatively new subprocesses not present at the Born level *i.e.* they do not possess singular configurations of partons which contribute to the dressing up of the distribution (fragmentation) functions already present in the Born term.
- $\Rightarrow$ These graphs (with a trigger on the g or q but *not* on q') are the lowest order BFKL terms in which extra gluons are emitted by the t-channel gluon
- These, therefore contribute precisely to the forward cross section that HERA experiments are supposed to study to reveal BFKL dynamics
- For example, for graph (b) with a forward trigger on q, cross section is seven times larger than the one corresponding to a trigger on q' ($x_{Bj} \sim 2.10^{-4}$)

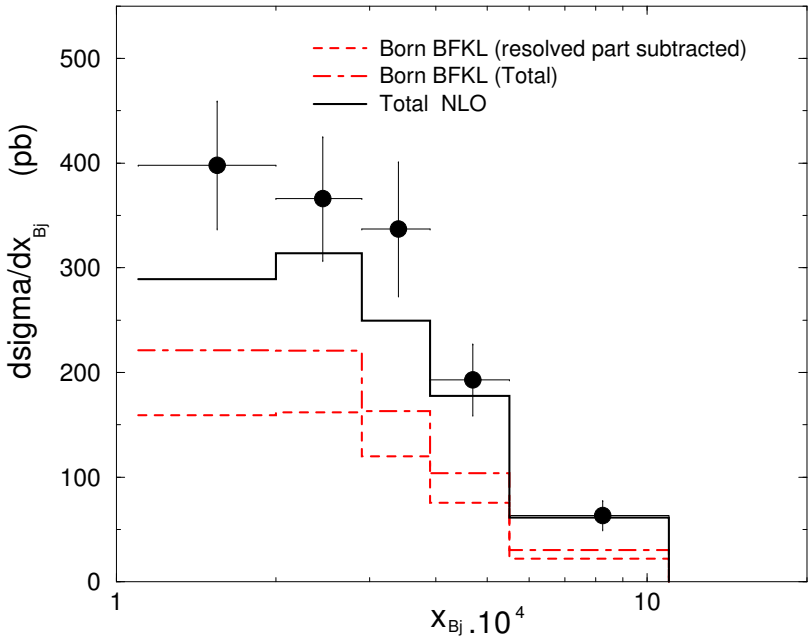

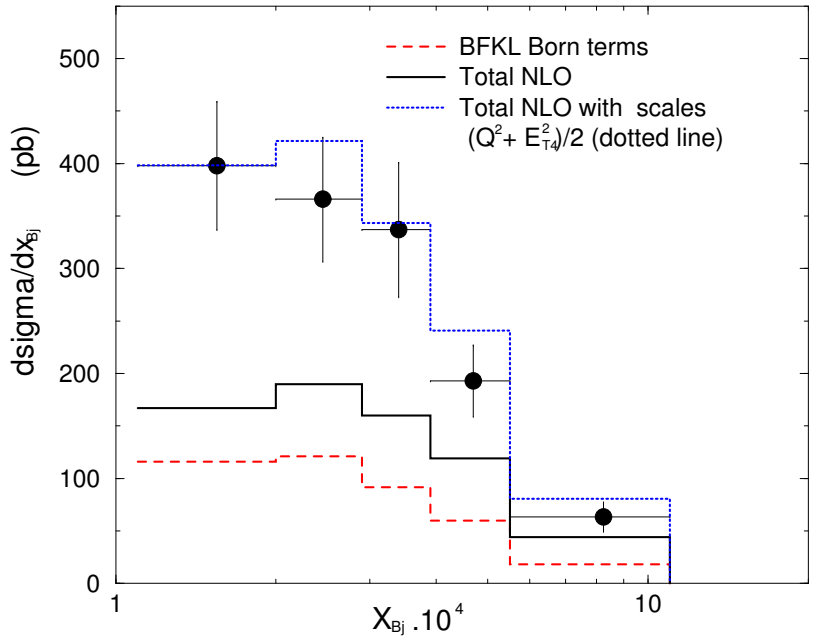

The BFKL Born contribution is more than two thirds of the total NLO correction.

$\Rightarrow$ Main part of the forward cross section is due to the BFKL Born terms ($\gamma^* q \longrightarrow q' \bar{q}' q$ and $\gamma^* q \longrightarrow q \bar{q} g$).

$\Rightarrow$ these channels are therefore strongly dependent on renormalization and factorization scales.

$\Rightarrow$ There is room for a BFKL-ladder contribution between data and present theoretical predictions if scale $M \sim p_T^{parton}$ but not with the more realistic $M \sim p_T^{hadron}$

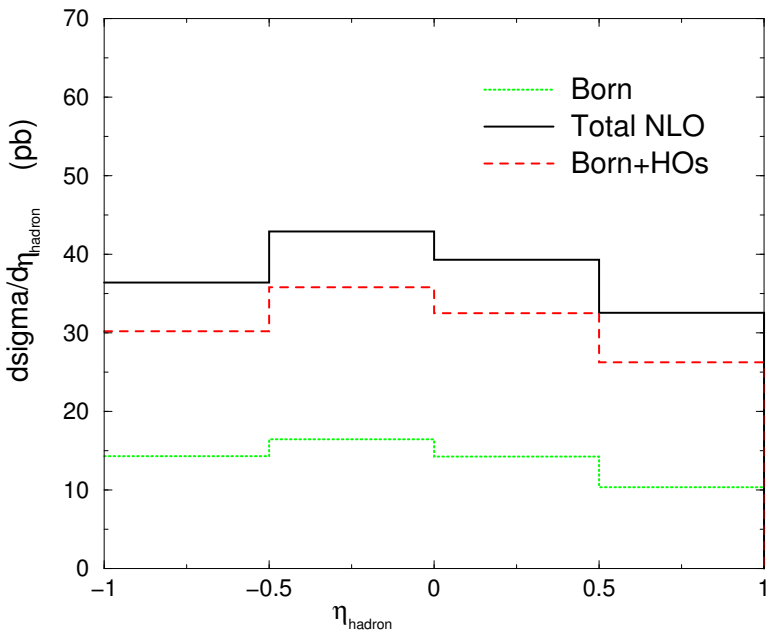

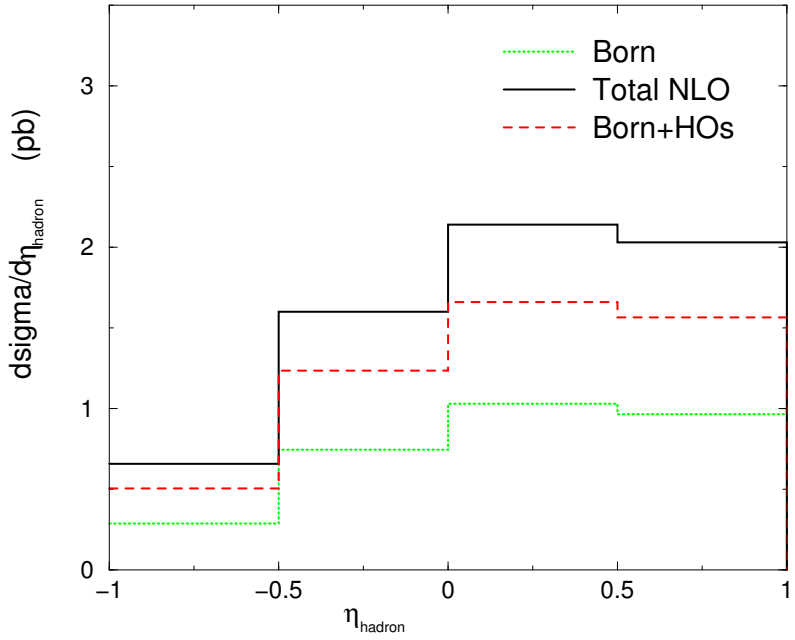

$d\sigma/d\eta_{hadron}$ large-$E_\perp$ π^0 cross section integrated over $E_\perp$ with cuts $E_\perp > 3$ GeV and $E_\perp > 7$ GeV. $\sqrt{S_{ep}} = 300$ GeV, $.3 \leq y \leq .7$ and $-1 \leq \eta_{hadron} \leq 1$:
5 GeV$^2 \leq Q^2 \leq 10$ GeV^2

- The ratio $r = \frac{HO_s}{Born}$ *decreases* as the cut on $E_\perp$ increases

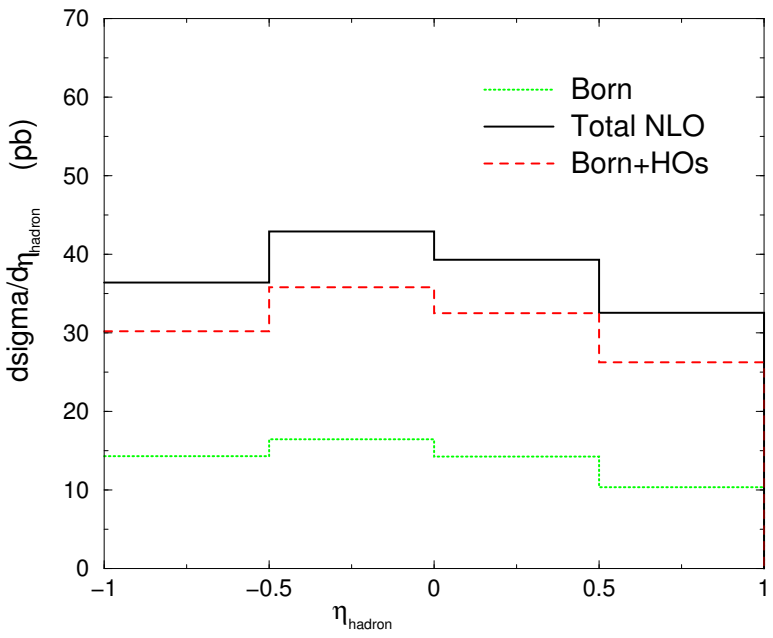

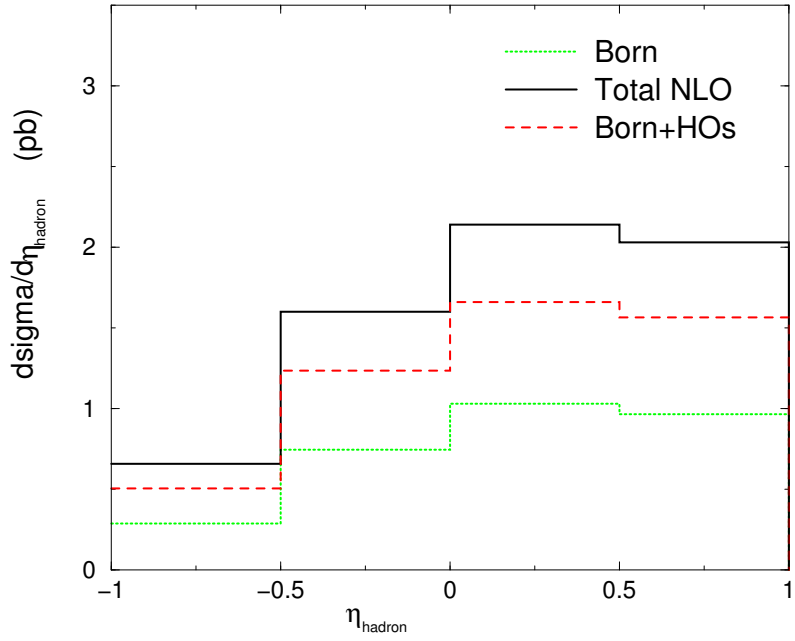

$d\sigma/d\eta_{hadron}$ large-$E_\perp$ π^0 cross section integrated over $E_\perp$ with cuts $E_\perp > 3$ GeV and $E_\perp > 7$ GeV. $\sqrt{S_{ep}} = 300$ GeV, $.3 \leq y \leq .7$ and $-1 \leq \eta_{hadron} \leq 1$:
5 GeV$^2 \leq Q^2 \leq 10$ GeV^2

- The ratio $r = \frac{HO_s}{Born}$ *decreases* as the cut on $E_\perp$ increases
- The ratio of the resolved contribution to the Born *increases* as cut on $E_\perp$ increases $\Rightarrow$ because of larger value of $(Q^2 + E_\perp^2)/Q^2$

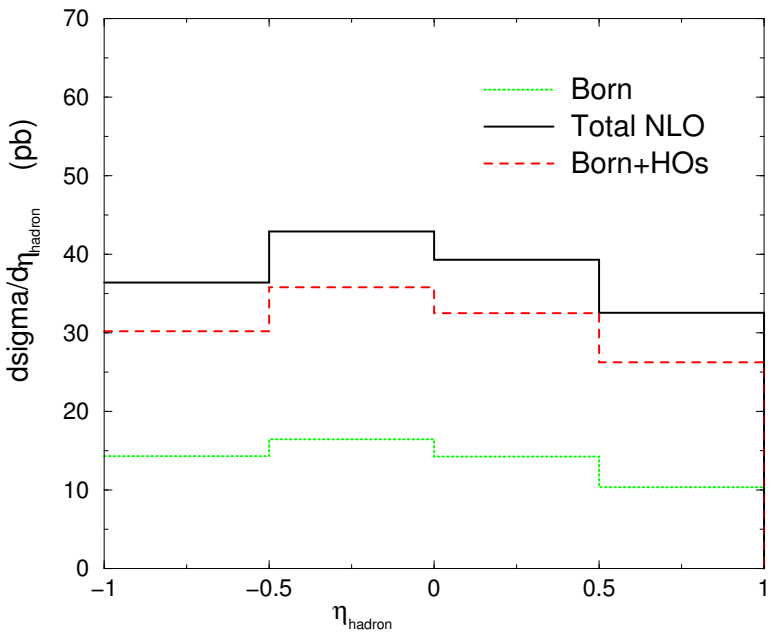

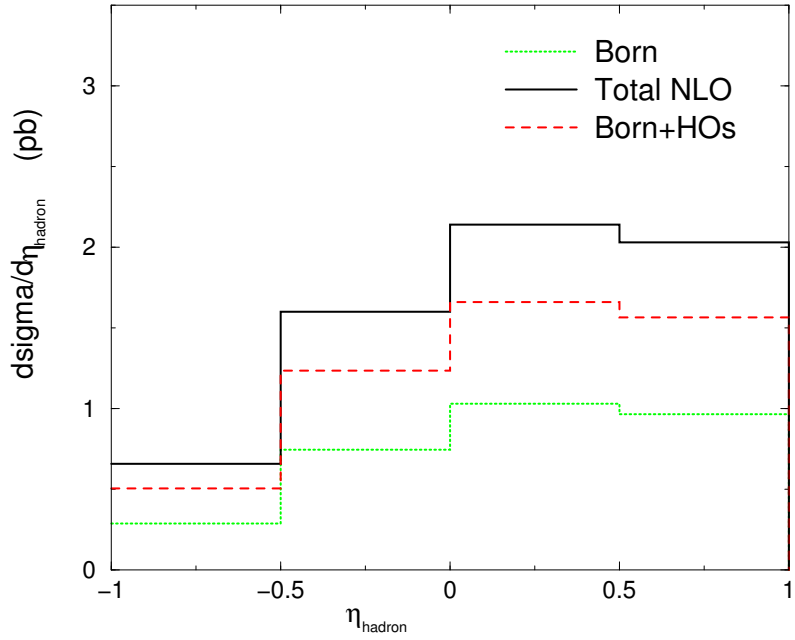

$d\sigma/d\eta_{hadron}$ large-$E_\perp$ π^0 cross section integrated over $E_\perp$ with cuts $E_\perp > 3$ GeV and $E_\perp > 7$ GeV. $\sqrt{S_{ep}} = 300$ GeV, $.3 \leq y \leq .7$ and $-1 \leq \eta_{hadron} \leq 1$:
5 GeV$^2 \leq Q^2 \leq 10$ GeV^2

- The ratio $r = \frac{HO_s}{Born}$ *decreases* as the cut on $E_\perp$ increases
- The ratio of the resolved contribution to the Born *increases* as cut on $E_\perp$ increases $\Rightarrow$ because of larger value of $(Q^2 + E_\perp^2)/Q^2$
- In photoproduction, this ratio is much larger. since the virtuality of the photon suppresses the resolved contribution

Scale dependence of the cross section

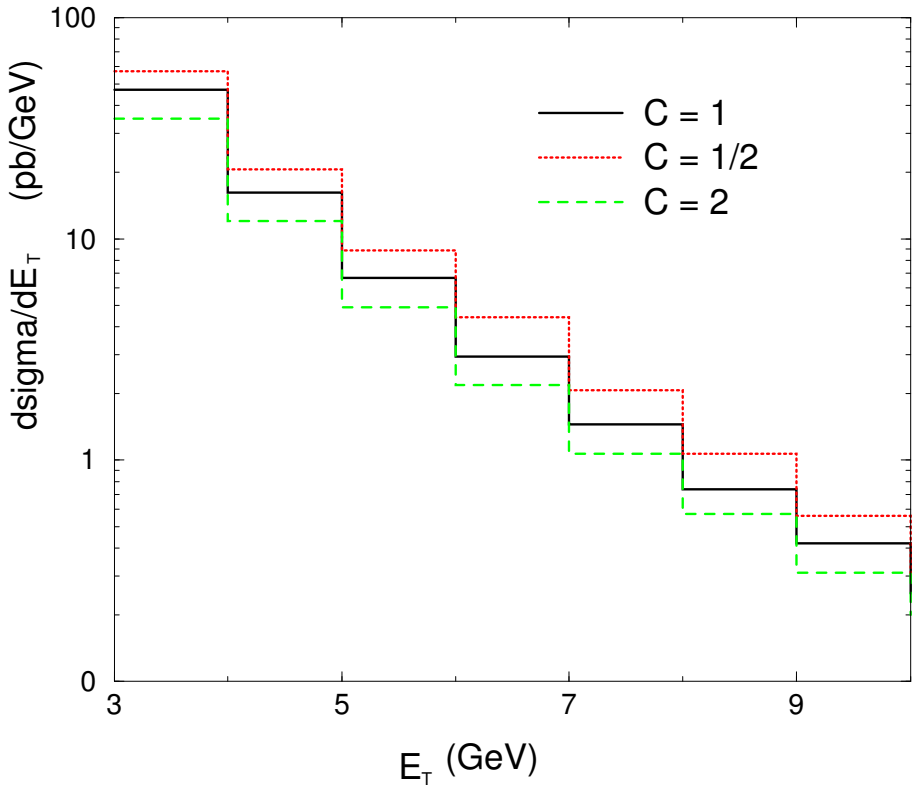

We use scales $\mu = M = M_F = C\sqrt{Q^2 + E_\perp^2}$ with $C = \frac{1}{2}, 1, 2..$

A change of scales by a factor 4 results in a change of cross section by a factor 2 $\Rightarrow$ even at large $E_\perp$ cross section very sensitive to scales.

Conclusions

- Carried out HO corrections to lepto-production cross section for large $E_\perp$ hadrons
- In the central region, large HO corrections at low $E_\perp$. These decrease as $E_\perp$ increases with $K(= HO/(HO + Born)) \simeq 0.5$.
- In the same range, HO corrections contain a non-negligible resolved contribution
  $\Rightarrow$ should allow experiments to constrain the virtual photon structure function.
- In the forward region, large HO corrections due to the opening up of the BFKL Born terms
  $\Rightarrow$ two-thirds of the NLO cross section is due to these contributions!
- The existence of these Born terms make the total NLO cross section quite sensitive to scale variations
  $\Rightarrow$ no absolute normalisation of the cross section possible – however good agreement between data and experiment with normalisation and factorisation scale $\simeq \sqrt{(Q^2 + E_\perp^2)/2}$.
- The scale sensitivity prevents any firm conclusion regarding importance of BFKL resummation in the forward cross section as measured by the H1 collaboration – would require NNLO corrections to the leptoproduction cross section.